Evaluation of a spatial rainfall generator for generating high resolution precipitation projections over orographically complex terrain

Corrado Camera[1], Adriana Bruggeman[1], Panos Hadjinicolaou[1], Silas Michaelides[1, 2], Manfred A. Lange[1]

[1] Energy, Environment and Water Research Centre, The Cyprus Institute, Aglantzia, Nicosia, 2121, Cyprus

[2] Cyprus Department of Meteorology, Nicosia, 1418, Cyprus

Corresponding author: Corrado Camera
Email: c.camera@cyi.ac.cy
Telephone: +357 22208691
Fax: +357 22208625

Abstract

Space-time variability of precipitation plays a key role as driver of many environmental processes. The objective of this study is to evaluate a spatiotemporal (STG) Neyman-Scott Rectangular Pulses (NSRP) generator over orographically complex terrain for statistical downscaling of climate models. Data from 145 rain gauges over a 5,760-km^2 area of Cyprus for 1980-2010 were used for this study. The STG was evaluated for its capacity to reproduce basic rainfall statistical properties, spatial intermittency, and extremes. The results were compared with a multi-single site NRSP generator (MSG). The STG performed well in terms of average annual rainfall (+1.5% in comparison with the 1980-2010 observations), but does not capture spatial intermittency over the study area and extremes well. Daily events above 50 mm were underestimated by 61%. The MSG produced a similar error (+1.1%) in terms of average annual rainfall, while the daily extremes (>50-mm) were underestimated by 11%. A gridding scheme based on scaling coefficients was used to interpolate the MSG data. Projections of three Regional Climate Models, downscaled by MSG, indicate a 1.5% to 12% decrease in the mean annual rainfall over Cyprus for 2020-2050. Furthermore, the number of extremes (>50-mm) for the 145 stations is projected to change between -24% and +2% for the three models. The MSG modelling approach maintained the daily rainfall statistics at all grid cells, but cannot create spatially consistent daily precipitation maps, limiting its application to spatially disconnected applications. Further research is needed for the development of spatial non-stationary NRSP models.

Keywords: gridded data sets; meteorological data; rainfall generator; statistical downscaling

1 Introduction

To downscale General Circulation Models (GCMs), two general approaches are available: dynamical downscaling and statistical downscaling. Dynamical downscaling involves the use of Regional Climate Models (RCMs), forced at the boundaries by GCM outputs, but characterized by a more detailed resolution, a limited area domain (e.g., Europe), and a higher capability in reproducing the physics of the processes (Rummukainen 2010). Recent projects such as ENSEMBLES (van der Linden and Mitchell 2009) brought the horizontal resolution of these models down to 25 km, and the CORDEX project (http://wcrp-cordex.ipsl.jussieu.fr/) is currently producing climate model results at 12.5 km resolution. On small domains (e.g., Western or Eastern Mediterranean Basin), experiments have already been carried out with resolutions of 10 km or lower (Gonçalves et al. 2014). However, these downscaling methods are computationally very intensive and may still not obtain a sufficiently high resolution (~1 km^2) for all applications (e.g. hydrological, agricultural and natural ecosystems studies, Avellan et al. 2012; Kizza et al. 2012; Supit et al. 2012; Parkes et al. 2013). Statistical downscaling links GCMs or RCMs to local climate by means of statistical models. According to Fowler et al. (2007), statistical downscaling approaches can be divided into three main groups - regression models, weather typing schemes, and weather generators – all relying on the assumption that local climate variables are a function of large scale atmospheric variables. These downscaling methods do not consider the physics of the processes but they can usually be applied for impact studies without the need of an additional bias correction step (Boé et al. 2007; Fowler et al. 2007); also, they are computationally less expensive, and allow working with finer resolutions. In particular, studies developing and applying weather generators are becoming increasingly common (e.g., Kilsby et al. 2007; Burton et al. 2008; Morlan and Burlando 2008; Wilks 2009; Burton et al. 2010a; Kleiber et al. 2012; Mehrotra et al. 2015).

Rainfall generators exist for both single site and spatial applications and three main categories of rainfall generators can be recognized (Bordoy and Burlando 2014). The first category is the one of the Markovian models, in which rainfall occurrence and rainfall amount are modelled separately in a two-step approach (Wilks 1998; Mehrotra et al. 2006; Kim et al. 2008; Wilks 2009). Rainfall occurrence is conditioned on the wet/dry state of the previous time steps, while rainfall amounts can be calculated with parametric methods based on rainfall probability distribution functions (Brisette et al. 2007; Khalili et al. 2009; Baigorria and Jones 2010), and non-parametric approaches employing resampling techniques like kernel density estimators (Harrold et al. 2003; Mehrotra et al. 2015) and k-nearest neighbour bootstrapping (Yates et al. 2003; Apipattanavis et al. 2007; Caraway et al. 2014). Particular parametric approaches, which allow incorporating covariates and large scale information into the stochastic generation process, are those based on the Generalized Linear Model (GLM) theory (Chandler and Wheater 2002; Yang et al. 2005; Kleiber et al. 2012), and weather states (hidden Markov chain models, e.g. Mehrotra et al. 2004; Moron et al. 2008). Most of the spatial (multi-site) approaches in this category of rainfall generators are based on transformations of the multivariate Gaussian distribution with the inclusion of a site to site correlation structure (e.g., Ailliot et al. 2009). Mehrotra et al. (2015) proposed an alternative approach to model the spatial dependence based on uniform random variates independent in time, but correlated in space. Specific problems of the Markovian approaches are the limits in reproducing extended drought periods due to the short memory (few time steps) of the occurrence modelling scheme (Maraun et al. 2010); and for the resampling schemes, to generate rainfall patterns outside the observation domain (Burton et al. 2010a)

The second category is that of models based on cluster processes such as Barlett-Lewis Rectangular Pulses (BLRP) models and Neyman-Scott Rectangular Pulses (NSRP) models (Rodriguez-Iturbe et al. 1987; Cowpertwait 1995; Cowpertwait et al. 2013). These models handle occurrence and amount in a single process. BLRP and NSRP (parametric) models are based on the arrival of storms as Poisson processes with characteristic timescales. Each storm is made up of a cluster of (a random number of) rain cells. The difference between the two models is the way in which a time position is attributed to the cells (Rodriguez-Iturbe et al. 1987). When modelling rainfall as a spatial phenomenon, the cluster of cells is built as a uniform Poisson process in space with a certain density of cell centres. Given their formulation, the models are not expected to exhibit scaling behaviour (e.g., Marani 2003). However, Olsson and Burlando (2002), Bordoy and Burlando (2014) empirically demonstrated that a NSRP model can well reproduce rainfall properties at different timescales, applying both its single site (20 min – 1 week) and spatial-temporal configuration (1h – 45 days). Another advantage of this type of models is the possibility to include third-order moments in the simulation algorithm to better model extremes (Burton et al. 2008). Conversely, a limitation of these models is that rainfall properties, excluding mean and variance, are invariant (Fowler et al. 2005). To overcome spatial stationarity issues, Burton et al. (2010a) presented an extension of the spatiotemporal NSRP model that allows a non-homogeneous spatial activation of rain cells. This modelling scheme is a good instrument to reproduce the spatial heterogeneity of rainfall statistics over complex terrains. However, the model is not easily adaptable to case studies with a large number of observational stations. Another spatiotemporal model based on rain cells and cell cluster processes for generating rainfall timeseries at the small spatial scale (100 to 1,000 km^2) has been proposed by Willems (2001). This model has mainly been applied for urban flood studies (e.g. Simões et al. 2015) and has been recently adapted to work with radar data (McRobie et al. 2013).

The third category is the one of disaggregation models, which couple the stochastic approach (e.g., log-Poisson stochastic generator in Mascaro et al. 2013) with scale invariant or multiscale properties recognized in the spatial-temporal pattern of precipitation (Veneziano et al. 2006; Morlan and Burlando 2008; Groppelli et al. 2011). Disaggregation methods are based on the assumption that rainfall is a multifractal scale invariant process inheriting its scaling properties from external forcing, usually atmospheric turbulence (Perica and Foufoula-Georgiou 1996; Deidda et al. 1999; Badas et al. 2006; Venugopal et al. 2006). The spatial variability of rainfall is modelled through multifractal cascades (Groppelli et al. 2011; Gires et al. 2012; Langousis et al. 2013; Mascaro et al. 2013). If multifractality is demonstrated, the major advantages are related to the light parameterization and a rather simple probabilistic structure of the model (Veneziano et al. 2006). However, these authors demonstrated that a multifractal, scale invariant, spatial-temporal pattern of rainfall cannot always be recognized, implying the necessity of an extensively parameterized scaling approach for rainfall or the need to define the link to atmospheric turbulence in a different manner (e.g., passing through water vapour condensation rates).

In general, the major challenges related to rainfall generators consist in developing efficient, easy to parameterize, spatial models able to work in any topographic environment (Burton et al. 2010a; Caraway et al. 2014) and to capture the properties of the extremes (Hashimi et al. 2011; Costa et al. 2015; Verdin et al. 2015).

The focus of the present study is on NSRP models. The choice was driven by the advantages related to the elegance of the model (limited number of parameters and fitting through observed time series), the inclusion of third order moments to model extremes, and the wide use of this type of models in the literature, which has demonstrated their robustness and adaptability to work in different climates and environments (e.g., Van Vliet et al. 2012; Borgomeo et al. 2014; Forsythe et al. 2014). The only study, which has made a thorough evaluation of a spatiotemporal NSRP model over a mountainous area, is the one of Bordoy and Burlando (2014). These authors tested the model in an alpine catchment in Switzerland

(5,244 km^2) for 10 reference rain gauges. Their conclusions suggest that the model can reproduce the main spatial and temporal rainfall characteristics well, with some limitations regarding the dry and wet spells durations and the modelling of extremes in the driest regions. In addition, no particular weaknesses appear in comparison with the single site version of the same model, as evaluated in Olsson and Burlando (2002).

The main goal of this study is to evaluate the performance of a spatiotemporal NRSP rainfall generator for the downscaling of precipitation from RCMs over orographically complex terrain with a dense rain gauge network. We apply the spatiotemporal NSRP model (RainSim V3.1.1, Burton et. 2008) for 145 rain gauges (period 1980-2010) over the 5,760 km^2 area under the effective control of the government of the Republic of Cyprus. The evaluation considers basic rainfall statistical properties, rainfall spatial and temporal (lag 1) intermittency, and indices of extremes. While our study area size is almost the same as that of Borday and Burlando (2014), the analysis of 145 gauges, as compared to their 10 stations, allows a much better analysis of the capacity of the spatiotemporal model to simulate spatial differences as well as a quantification of the loss of model capacity under specific geographical conditions. We also conduct a direct comparison between the output of the spatiotemporal model and the output of a single site generator for the 145 gauges. Two different spatial interpolation methods are used to create high-resolution gridded datasets (1 x 1 km^2) for the two model applications. Finally, climate change projections of three RCMs (A1B scenario) are downscaled and interpolated for Cyprus (2020-2050).

The area under the control of the Republic of Cyprus (5,760 km^2) is an interesting case study because its complex topography strongly affects the spatial patterns of the different meteorological variables. It has also experienced an increase in the number of drought years in the recent past (Michaelides et al. 2009). In addition, it is also expected to be a hot spot for climate change (Lelieveld et al. 2012).

2 Methods

The present study consists of the following steps: i) the evaluation of a spatiotemporal NSRP rainfall generator (STG) and its gridded product for the period 1980-2010 and comparison with outputs obtained from a multi-single site version (MSG) of the same model; ii) a precipitation downscaling application for Cyprus with the creation of gridded projections (1 x 1 km^2) for the period 2020-2050. These steps are presented in the following sub-sections.

2.1 Evaluation of the spatial-temporal rainfall generator

The RainSim V3.1.1 software (Burton et al. 2008) was used to generate rainfall time series. RainSim is an NSRP model based software, applicable both at a single site and in spatial-temporal mode. It takes into consideration third moment properties, which are important to calculate extremes. The model includes two parts: i) a spatially homogeneous and time stationary Poisson process that models the arrival of rainfall events and their mean characteristics (duration and intensity); ii) a spatially non-homogeneous field, proportional to the mean rainfall, describing intensity scaling factors. The software has three main steps: i) analysis of the observed data to calculate the statistics to fit the model; ii) fitting of the model parameters based on the observed rainfall statistics; iii) generation of time series. Five parameters must be fitted by the model for point applications and seven for spatial-temporal applications (Table 1).

Seven daily statistics were used to fit the model parameters for each month (both spatiotemporal and single site): mean, variance, skew, lag-1 autocorrelation, probability of dry days (threshold 0.2 mm), probability of consecutive dry days, and probability of consecutive wet days. The statistics were calculated for all 145 rainfall stations. To use the software in its spatial-temporal configuration, a matrix of lag-0 cross-correlation coefficients between each pair of stations was also calculated. The statistics were derived using the analytical module of RainSim for each of the 12 months of the year.

Table 1. Parameters of the Neymann-Scott Rectangular Pulses model for rainfall time series generation (Burton et al., 2008).

Parameter	*Description*	*Model*	*Units*
λ^{-1}	Mean time between adjacent storm origins	Point/Spatial	[h]
β^{-1}	Mean waiting time for raincell origins after storm origins	Point/Spatial	[h]
η^{-1}	Mean duration of raincell	Point/Spatial	[h]
N	Mean number of raincells per storm	Point	[-]
γ^{-1}	Mean radius of raincells	Spatial	[km]
P	Spatial density of raincell centres	Spatial	[km^{-2}]
ξ^{-1}	Mean intensity of a raincell	Point/Spatial	[mm/h]
Φ	A vector of scale factors, one for each raingauge	Spatial	[-]

To get the best set of model parameters, the fitting procedure implemented in RainSim V3.1.1 uses a numerical optimization algorithm to minimize the following objective function (Burton et al. 2008):

$$D(\lambda,\beta,...,\xi)=\sum_{g\in\Omega}\frac{w_g^2}{g_s^2}\left[\bar{g}-\hat{g}(\Theta)\right]^2 \qquad (1)$$

where Ω is the vector including the previously listed seven statistics, g denotes one of the statistics, w_g is the vector of the weights that can be used to assign a different importance to the statistics, g_s is the mean annual value of statistic g, $\bar{g}$ is the observed sample estimate, and $\hat{g}$ is the analytical expression of statistic g as a function of the model parameters (Cowpertwait et al. 2002; Bordoy and Burlando 2014). The value of g_s is set to 1 for the probability of a dry day, for the probability of consecutive dry/wet days, and for the spatial and temporal correlation. For further details about the software see Burton et al. (2008).

The STG was subsequently run to obtain daily simulated time series, 31-year long, for the past (1980-2010). To evaluate the general performance of the rainfall generator, the fitted and simulated statistics of the generated time series were compared to the statistics from observations. In addition, Kolmogorov-Smirnov and Anderson-Darling tests were performed to test the null hypothesis that the generated rainfall time series were samples from the same distributions of the observations. The first test gives an indication of the goodness of fit between two entire distributions (simulated and observed daily rainfall in this case), while the second test is designed to detect discrepancies in the tails of the distributions (Law and Kelton 1991). Specifically for extremes, some indices, independent from the rainfall simulation (i.e., statistics not used to fit the model), were calculated. The indices were selected and slightly modified from those presented by Zhang et al. (2005):

R20: the number of days (annual average) with precipitation higher than 20 mm;

R50: as R20 but with a threshold of 50 mm;

RT95: the threshold value (mm rain) at the 95th percentile of days with precipitation higher than 1 mm, for the whole 31-year long time series;

RT99: as RT95 but for the 99th percentile;

RA95: the annual mean of the total precipitation fallen on days with precipitation above RT95;

RA 99: as RA95 but for the 99th percentile.

In addition, for a further evaluation of the STG, the spatial intermittency (expressed as the number of wet rain gauges over the study area on a single day) of daily rainfall (precipitation > 0.2 mm) was calculated and compared for both the simulated and the observed time series. Summary statistics are presented for all 145 stations and more detailed comparisons for five representative stations. These stations (Figure 1) were selected on the basis of their geographical and topographical position, to cover regions with different rainfall regimes: station 41, Polis, representative of the north and west coast region; station 225, Prodromos, representative of the mountainous region of the Troodos; station 660, Kornos, representative of the foothills region; station 666, Athalassa-Nicosia, representative of the Mesaoria Plain region; and station 731, Larnaka, representative of the south and eastern coast.

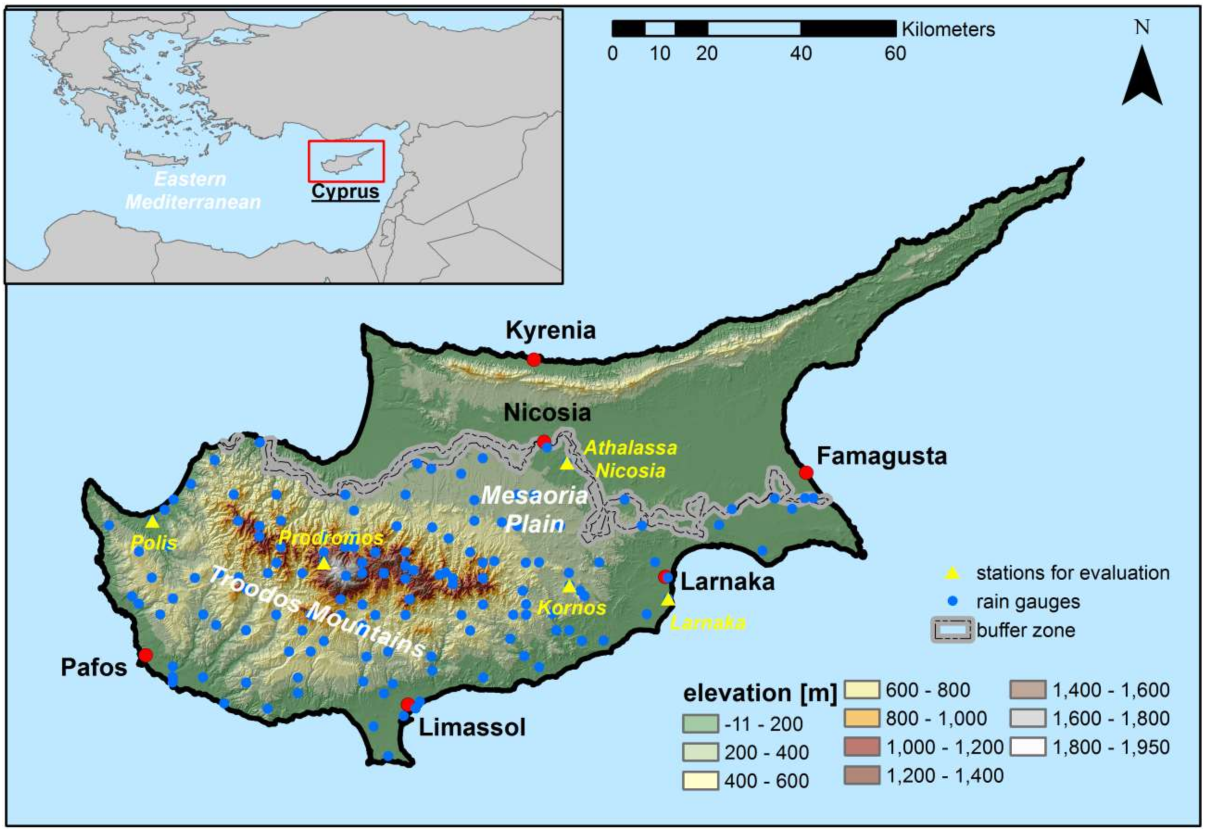

Fig. 1. The island of Cyprus with its main physical characteristics. The study area is located south of the buffer zone (shown by dashed lines). The location of the 145 rainfall stations is also shown, with the five stations used for the more detailed evaluation marked with triangles.

2.2 Gridding schemes

The spatial-temporal version of RainSim V3.1.1 (STG) accounts for spatial correlation, therefore, the daily time series simulated with this configuration can be spatially interpolated with common methods. The method developed and tested by Camera et al. (2014) to derive 1 x 1 km^2 daily gridded data sets of precipitation for Cyprus (1980-2010) was applied. The method involves inverse distance weighting (IDW) to interpolate local events, while a combination of step-wise geographically weighted regression and IDW is used for large scale events. The method was evaluated through a recursive cross validation scheme. The mean absolute error ranged from 0.08 mm for very low rainfall events (below the 30^{th} percentile), to 4.50 mm for extreme events (above the 85^{th} percentile). This gridding method, in the following text, is referred to as the two-step interpolation scheme (TSI).

The daily time series generated with the multi-single site version of RainSim (MSG) are not spatially correlated; therefore they cannot be interpolated with standard neighbouring techniques. Hence, a simplified gridding scheme is developed. Thiessen polygons are established around each observational station and raster cells, from the 1 x 1 km^2 mask map of the gridded data sets (Camera et al. 2014), are assigned to the different polygons. A scaling coefficient is calculated for each cell as the ratio between the mean annual rainfall (from observations 1980-2010) of the cell itself and the same value of the reference station, for the Thiessen polygon in which they fall. Each daily value is then calculated at each cell by multiplying the value from the generated time series at the station of reference for the scaling coefficient. Because the rainfall generator is parameterized on a monthly basis, accumulated monthly and annual precipitation values are spatially consistent. However, daily precipitation is not. In the following, this gridding method is referred to as the scaling coefficient interpolation scheme (SCI).

2.3 Future projections

Six different RCMs from the EU ENSEMBLE project database (http://ensemblesrt3.dmi.dk/), the same as in Hadjinicolaou et al. (2011), were selected as sources for future precipitation data. The models were evaluated for their capabilities of reproducing Cyprus climatology before being downscaled. The downscaling was carried out with a two-step approach: first change factors (Prudhomme et al. 2002) were calculated from the RCMs for daily rainfall statistics on a monthly base and then used to derive projected future time series at the rain gauges locations (Kilsby et al. 2007; Burton et al. 2010b). In the second step, these statistics were used as input in RainSim V3.1.1 to simulate future time series. The methods for the evaluation of the RCMs and the downscaling equations are presented in the supplementary material (Online Resource 1).

To evaluate changes in the rainfall regime between the future time-span (2020-2050) and the reference period (1980-2010), average annual rainfall values were compared. In addition, changes in the same indices of extremes used in the rainfall generator evaluation step (R20, R50, RT95, RT99, RA95, and RA99) were computed.

3 Results

3.1 Evaluation of the rainfall generator

In Fig. 2 and Fig. 3 scatter plots are displayed showing the comparison between observed and simulated mean daily rainfall (mean), daily variance (var), daily skew (skew), lag-1 autocorrelation (autocorr), percentage of dry days (pdry), and percentage of consecutive wet days (pww) for STG and MSG. The daily mean is very well modelled by both configurations of the rainfall generator, as the values aligned along the bisector show. Variance is fairly well modelled by both configurations as well. During wet winter months, the STG shows a little higher dispersion of the points around the bisector than the MSG, while both configurations show a clustering around very low values during the dry summer months. Skew is, on the contrary, much better modelled by the MSG than by the STG. The STG shows a horizontal clustering of the skewness values almost for every month, indicating that the model is smoothing out skew characteristics over the study area. In addition, for both configurations of the rainfall generator, the skew shows its largest dispersion in the very dry period (June-August). This is obviously due to the few events that characterize the summer months and the resulting high influence of these events on this statistic. However, considering that there are few rainy days and generally low rainfall amounts in summer, these errors can be considered negligible.

For the STG, lag-1 autocorrelation is showing a mixture of horizontal clustering (prevalent in wet months) and high dispersion (prevalent in dry months) resulting in a fairly poor modelling of this statistic. Conversely, although still showing some errors in the driest months (May-September), the MSG is generally able to reproduce lag-1 autocorrelations well. Percentage of dry days, consecutive dry days (not shown because it is very similar to pdry), and consecutive wet days are very well modelled by the MSG, while the spatial

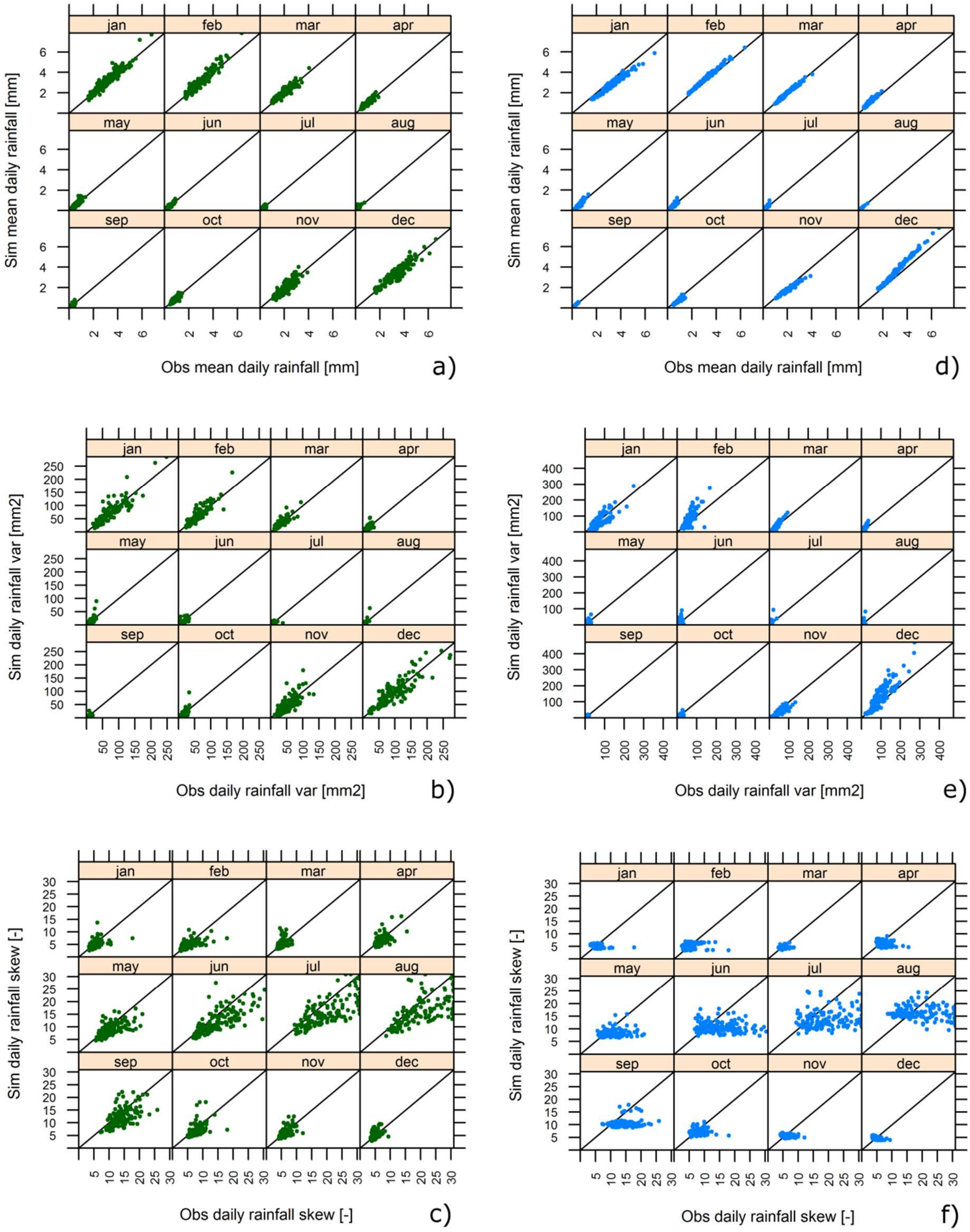

Fig. 2. Comparison of observed and simulated rainfall statistics for single site (a, b, c) and spatial rainfall generator (d, e, f) for 145 stations: mean daily rainfall (a, d); daily variance (b, e); daily skew (c, f). The statistics are calculated and presented on a monthly basis.

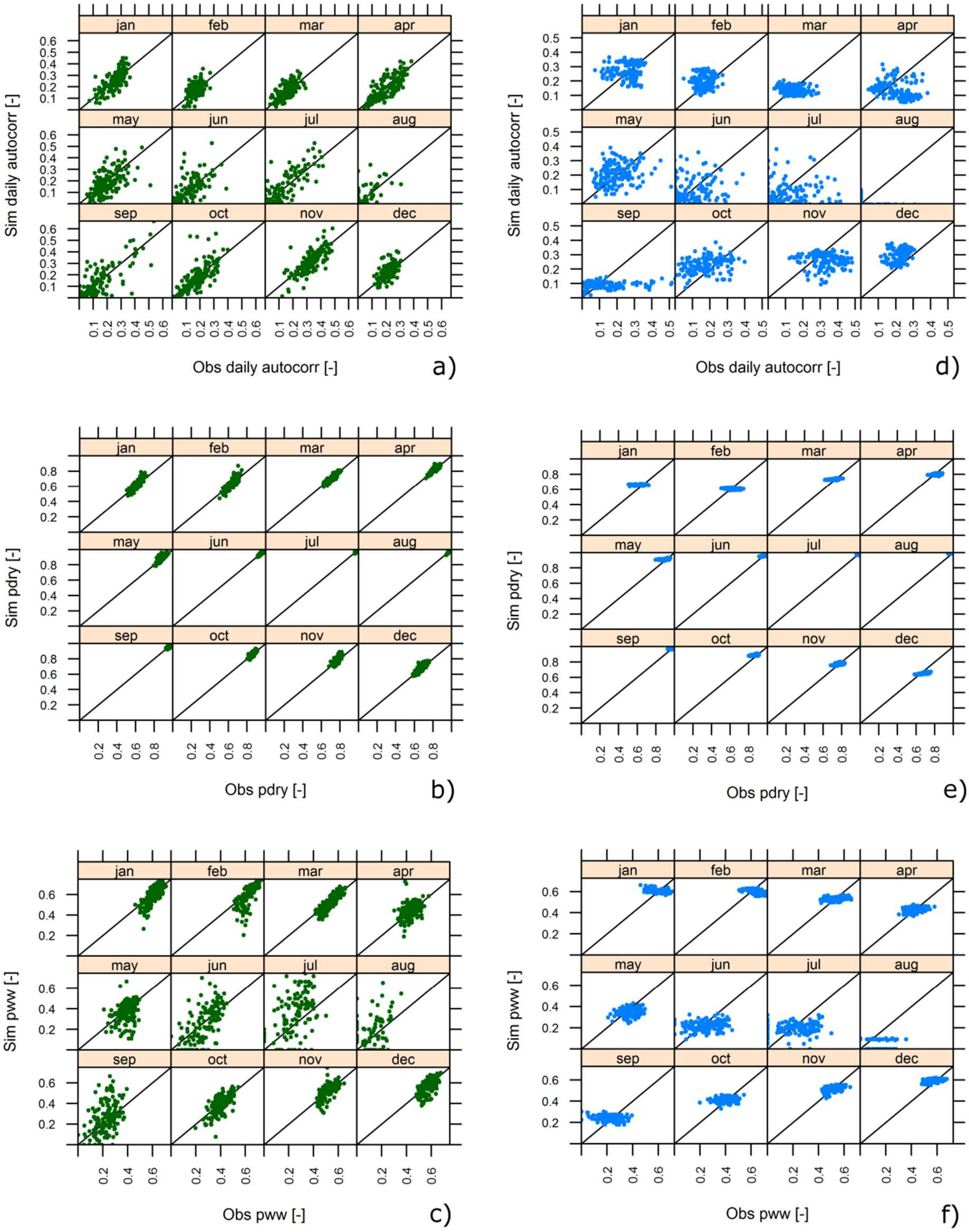

Fig. 3. Comparison of observed and simulated rainfall statistics for single site (a, b, c) and spatial rainfall generator (d, e, f) for 145 stations: lag-1 autocorrelation (a, d); percentage of dry days (b, e); and percentage of consecutive wet days (c, f). The statistics are calculated and presented on a monthly basis.

version shows a tendency to cluster all the modelled stations for a given month around the same value (horizontal clusters like for skew and autocorrelation). This poor differentiation between the stations' simulated statistics is the result of the fitting procedure of the model parameters. As briefly explained in the introduction, the spatiotemporal model is based on a homogeneous Poisson's process, which leads to constant fitted values, over the whole study area, of all the statistics except the mean and variance. Rainfall mean and variance vary across the study area, but the coefficient of variation remains uniform, as well as all the other rainfall statistics. The result is that mean and variance are usually well modelled at each location of interest but the other statistics (probability of a dry day, probability of consecutive dry and wet days, skew, and autocorrelation) remain constant all over the study area (Fowler et al., 2005). In a topographically uniform area, this may be an acceptable assumption, but in orographically complex regions, with different rainfall regimes, it can lead to large errors in the simulation of the statistics.

In Fig. 4, an example of the percentage of consecutive wet days is presented for the five representative stations. Observed, fitted and simulated statistic values for the 12 months are shown for both MSG and STG. The fitted statistics are calculated by the model while fitting its internal parameters (Table 1). The simulated statistics are calculated from the generated time series. Theoretically, the generation of an infinite long time series should give statistics equal to their fitted values. For the STG, all statistics, with the exception of mean and variance, are fitted on the average value of the study area for each month. This means, for example, that the value of the generic statistic S for month M at station N_x is equal to the value of the same statistic S, for the same month M, at any other station N_y over the study area. This simplification in the model fitting scheme influences also the simulated statistics (Fig. 4b) and therefore the distribution functions of the generated time series.

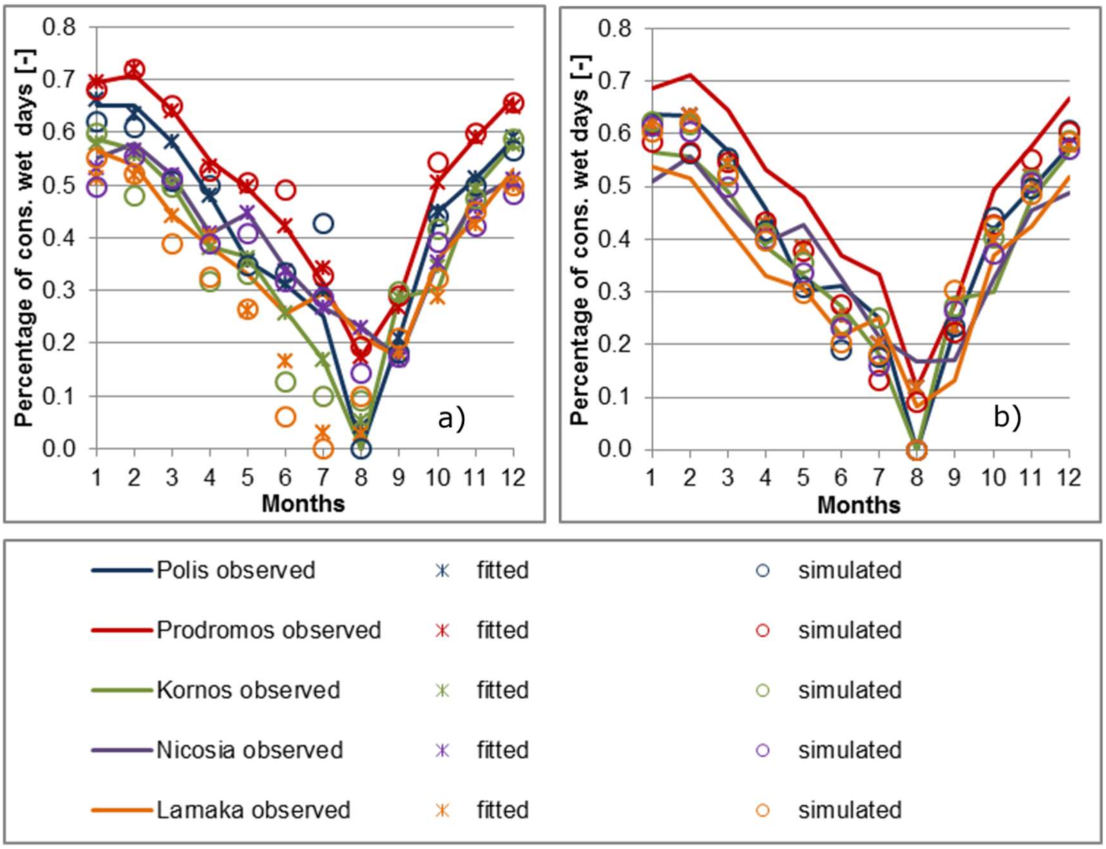

Fig. 4. Observed, fitted, and simulated percentage of consecutive wet days for the five stations of Fig. 1 plotted on a monthly basis: a) single site and b) spatial-temporal rainfall generator.

In Fig. 5, the results of the Kolmogorov-Smirnov and Anderson-Darling tests are shown. We rejected the null hypothesis of similarity of the distributions of simulated and observed time series for p-values lower than 0.01. The spatial analysis of the results of these tests shows two main outcomes. For the STG, for both tests, the null hypothesis is usually accepted at stations located in the foothills of the mountains, i.e. at those stations that are expected to have an average behaviour, and that can be better modelled by the average values of the statistics. The Anderson-Darling test (null hypothesis rejected at 118 stations for STG, and at 43 stations for MSG) appears more selective than the Kolmogorov-Smirnov test (null hypothesis rejected at 94 stations for STG, and at 10 stations for MSG) and emphasizes the weakness of the NSRP model (in its single site as well) in capturing extremes, especially in dry areas. With a p-value threshold of 0.05, the same general trend can be observed, with the only difference of the rejection of the null hypothesis, for the Anderson-Darling test, at all the stations located on the northern foothills of the Troodos Mountains for the STG model.

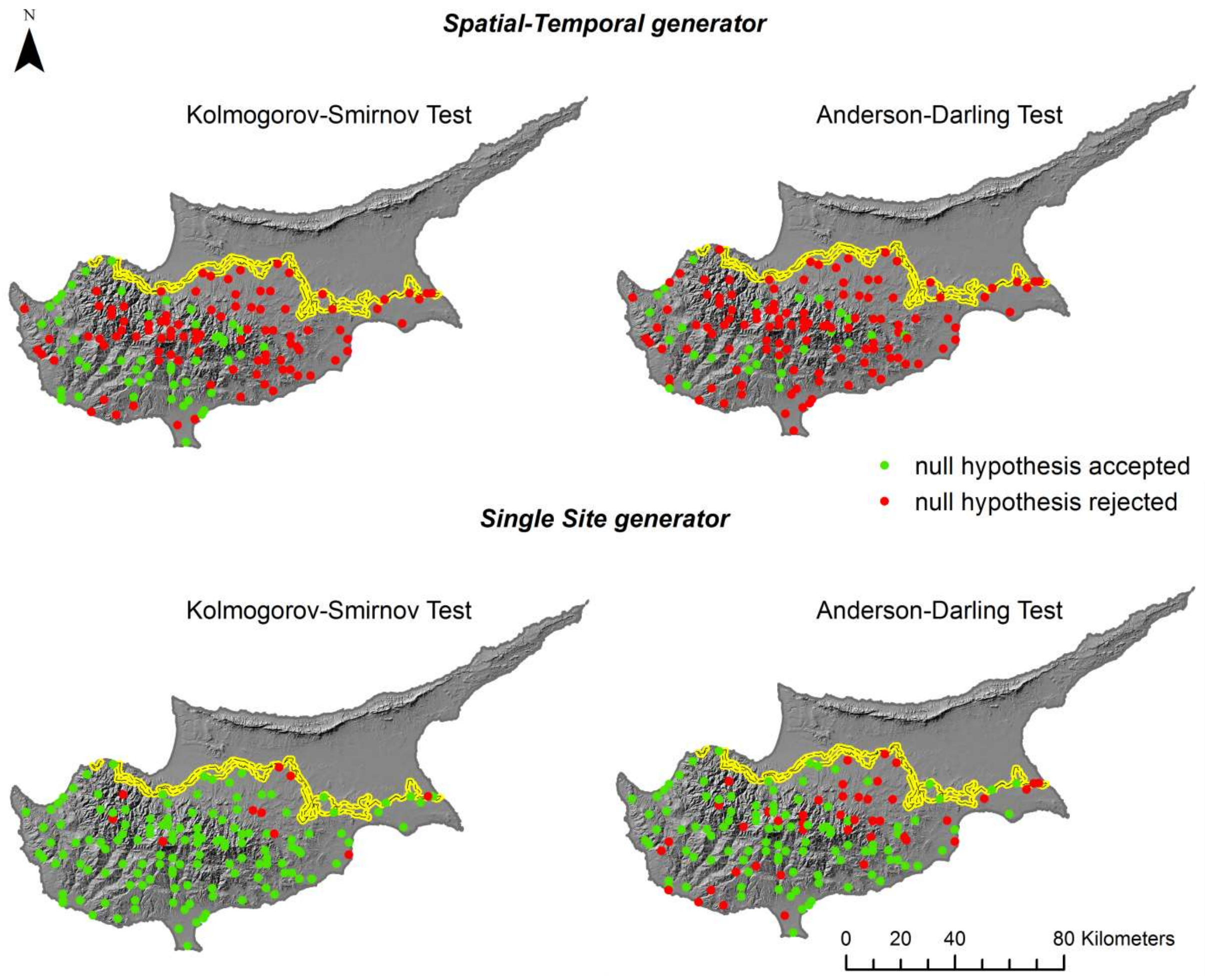

Fig. 5. Results of the Kolmogorov-Smirnov and Anderson-Darling tests performed to verify the null hypothesis of similarity of the distribution functions of simulated (through spatial temporal and single rainfall generator) and observed time series. The null hypothesis is rejected for p-values lower than 0.01.

This is demonstrated in Table 2 as well, where the indices R20, R50, RT95, RA95, RT99 and RA99 are plotted for both rainfall generator configurations, at the five representative stations. Also, Fig. 6 presents boxplots for every index (R20, R50, RT95, RT99, RA95, and RA99) showing the distribution of the relative error as calculated at the 145 rain gauges. The MSG performs very well in reproducing the values of the RT95 and RA95 indices, with mean and median errors over the 145 rain gauges between -2% and -3%, and errors at single stations usually lower than 10%, as it is testified by the very short inter quantile range (IQR). Conversely, the STG shows mean and median errors around -15% for the RT95 and around -20% for the RA95, also with much wider IQRs. The behaviour in terms of RT99 and RA99 is similar, for both model configurations, to the one shown for RT95 and RA95, with slightly higher mean and median errors and wider IQRs. Regarding the R20 and R50 indices, the two configurations perform similarly and sufficiently well over the wettest regions of the study area (e.g., Polis and Prodromos in Table 2), but the STG completely misses to reproduce these rainfall characteristics in the dry region (e.g. Kornos, Nicosia, Larnaka in Table 2). This reflects also in the shape of the boxplots in Fig. 6. In fact, the R20 and R50 inter quantile ranges calculated from the time series simulated with the STG are much wider than those calculated from the MSG time series, showing larger differences in the quality of the modelling at different rain gauges. Bordoy and Burlando (2014) observed a general good representation of extremes modelled by the STG over a 5,244 km^2 Swiss mountain catchment, with some limitations over the driest region. According to our results, the STG completely failed to model extremes over dry regions of an orographically complex study area. Therefore, extreme event modelling remains a crucial issue to be solved in the implementation of a spatiotemporal (NSRP) model, although the analysed observed and simulated 30-year periods may be too short to capture and represent extremes adequately. The introduction of the non-homogeneous spatial activation of rain cells (NSAR-NSRP) model by Burton et al. (2010a) can certainly bring advantages in terms of better modelling of rainfall statistics, overcoming the issue of spatial invariance. However, it still has to be demonstrated that this will result in better modelling of the extremes. Deriving a method combining the separate modelling of low values and extremes, as proposed by Costa et al. (2015), could be a valuable solution to try implementing in ST-NSRP models as well. Finally, the observed and simulated mean annual rainfall for 1980-2010 was compared at all 145 stations. The normalized mean absolute errors (simulated in comparison to observed values) are 3.6% and 1.4% for the MSG and the STG data, respectively.

Table 2. Comparison of observed (obs) and simulated (1980-2020) rainfall extremes (R20, R50, RT95, RA95, RT99, RA99) for single site (MSG) and spatial rainfall generator (STG) at five representative rain gauges.

Station ID:		41	225	660	666	731
Location:		Polis	Prodromos	Kornos	Athalassa	Larnaka
Elevation [m a.s.l.]		15	1380	370	162	1
$R20_{obs}$	**[day/yr]**	4.5	11.5	5.8	3.3	4.0
$R20_{MSG}$	**[day/yr]**	4.5	11.3	6.1	3.4	4.0
$R20_{STG}$	**[day/yr]**	4.2	13	4.2	1.7	1.9
$R50_{obs}$	**[day/yr]**	0.3	1.8	1.0	0.5	0.5
$R50_{MSG}$	**[day/yr]**	0.2	1.5	0.9	0.5	0.6
$R50_{STG}$	**[day/yr]**	0.2	1.6	0.2	0.0	0.0
$RT95_{obs}$	**[mm]**	26	39	34	26	29
$RT95_{MSG}$	**[mm]**	26	38	31	25	29
$RT95_{STG}$	**[mm]**	25	42	24	18	18
$RA95_{obs}$	**[mm]**	88	200	123	86	84
$RA95_{MSG}$	**[mm]**	83	186	120	84	100
$RA95_{STG}$	**[mm]**	84	161	92	60	59
$RT99_{obs}$	**[mm]**	44	72	69	53	52
$RT99_{MSG}$	**[mm]**	39	59	57	51	55
$RT99_{STG}$	**[mm]**	36	63	40	26	27
$RA99_{obs}$	**[mm]**	26	63	38	27	24
$RA99_{MSG}$	**[mm]**	24	57	37	28	36
$RA99_{STG}$	**[mm]**	23	46	28	16	17

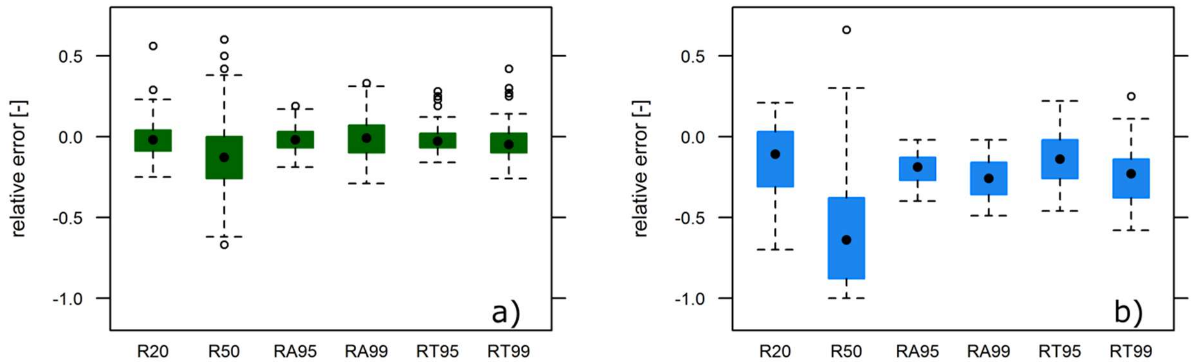

Fig. 6. Boxplots showing the distribution of the relative error [(simulated – observed)/observed] of the extreme rainfall indices (R20, R50, RT95, RT99, RA95, and RA99) at 145 rain gauges for a) single site rainfall generator, and b) spatial temporal rainfall generator. The boxes represent the interquartile range (IQR), the black dot inside the box is the median, whiskers extend 1.5·IQRs, the circles are the outliers.

The comparison between the spatial rainfall intermittency of the observed and simulated time series is plotted in Fig.7, showing the probability of having a certain number N of wet stations (≥ 0.2 mm) on any single day. The two distributions are bimodal, with the highest peak at the value of 0 stations, representing dry days all over the study area, and a second peak at the value of 145 stations, representing rainfall events that cover the whole study area. Both peaks are more pronounced for the simulated than for the observed data. Conversely, the STG produces much fewer small and medium scale events (< 80 rain gauges) than the observed series. Especially, the number of daily events occurring at a small number of stations (< 10) is much lower for the simulated than for the observed time series. In fact, it is easy to relate this evidence with the clustering, around the same value for all the stations, of the statistics reproducing the wet/dry state of the days. Thus, the main problem of the STG is its incapability to simulate small scale events.

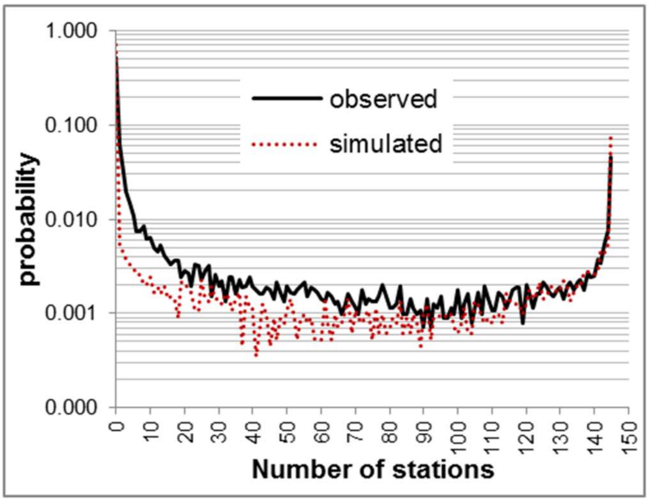

Fig. 7. Probability density functions of the number of stations that receive rain on any single day, for the observed and the simulated (spatial generator only) time series (1980-2010). A logarithmic scale is used.

3.2 Evaluation of gridded data sets

An example of two daily rainfall maps obtained with the two different combinations of downscaling and gridding methods is presented in Fig. 8. It is evident that the map obtained with the STG and a traditional interpolation scheme creates outputs that are spatially consistent and exhibit continuity in the precipitation over the study area. However, due to the demonstrated limitations of STG in reproducing extremes, these maps can be used only for application aiming at studying long term mean climatological characteristics (e.g., long-term mean annual runoff but not floods) and also in these cases the possible influence of extreme values on the average processes must be taken into consideration. On the contrary, the output calculated using the MSG and the simplified gridding schemes looks patchy and disconnected, clearly showing how cells are spatially continuous only within single Thiessen polygons. This means that the created daily data set can be used for any application in which cells can be analysed singularly (or as a group inside a single Thiessen polygon) but are not suitable for applications that require spatial connectivity. The use of this output is therefore limited to applications that do not involve spatial connection of areas located across different Thiessen polygons, such as distributed hydrologic modelling. In addition, the method is smoothing out rainfall variability inside each Thiessen polygon but it allows keeping the water balance over a monthly and annual scale. For plot-based applications such as crop modelling or ecological assessments, the MSG output is very useful and much better than the STG, due to its capacity to reproduce all precipitation statistics and properties.

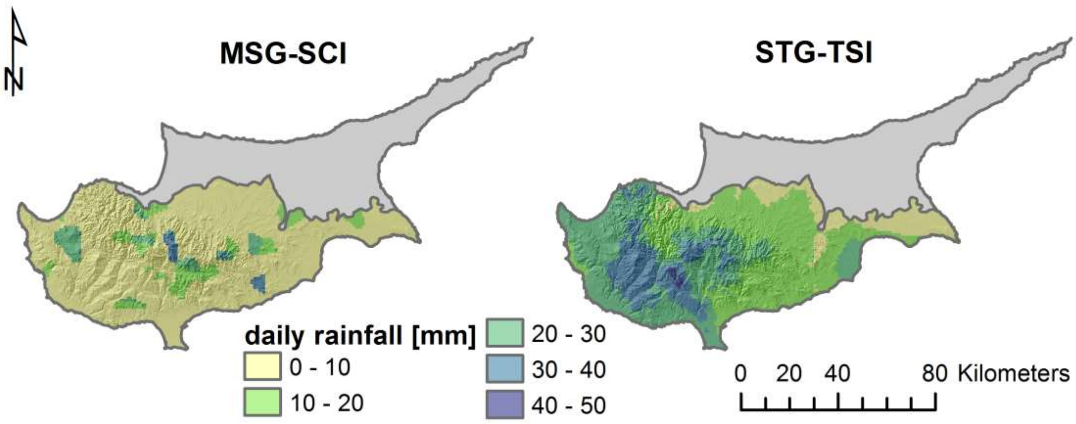

Fig. 8. Daily rainfall maps obtained with the two different methods: MSG-SCI (single site rainfall generator and scaling coefficients interpolation scheme), and STG-TSI (spatial temporal rainfall generator and two-step interpolation scheme). Both maps represent a winter day.

In Fig. 9, the gridded values of mean annual rainfall, calculated from observation and two groups of 145 simulated time series, are shown for the period 1980-2010. Observations are interpolated on a daily basis, with the two-step interpolation scheme (TSI). Simulated daily time series are obtained by running both a STG and a MSG and gridding is performed accordingly. The same general spatial variation of mean annual precipitation can be observed in the three maps, and confirmed by the very similar mean annual values over the whole country of the three data sets. The deviations from the observed mean annual rainfall are 1% and 1.5% for the MSG-SCI and the STG-TSI methods, respectively. However, increased short distance variability (e.g., higher mean annual rainfall values in the middle of an area characterized by very low values, as along the northern border of the study area) can be noticed for the MSG-SCI method, due to the independent generation of 145 – 31 years long – stochastic time series, and the resulting small, random (positive or negative) deviations from the input. However, the mean annual rainfall maps calculated with the two methods can be considered consistent with each other and with the observations. Therefore, both methods can be considered reliable and robust for projecting future changes of mean annual rainfall.

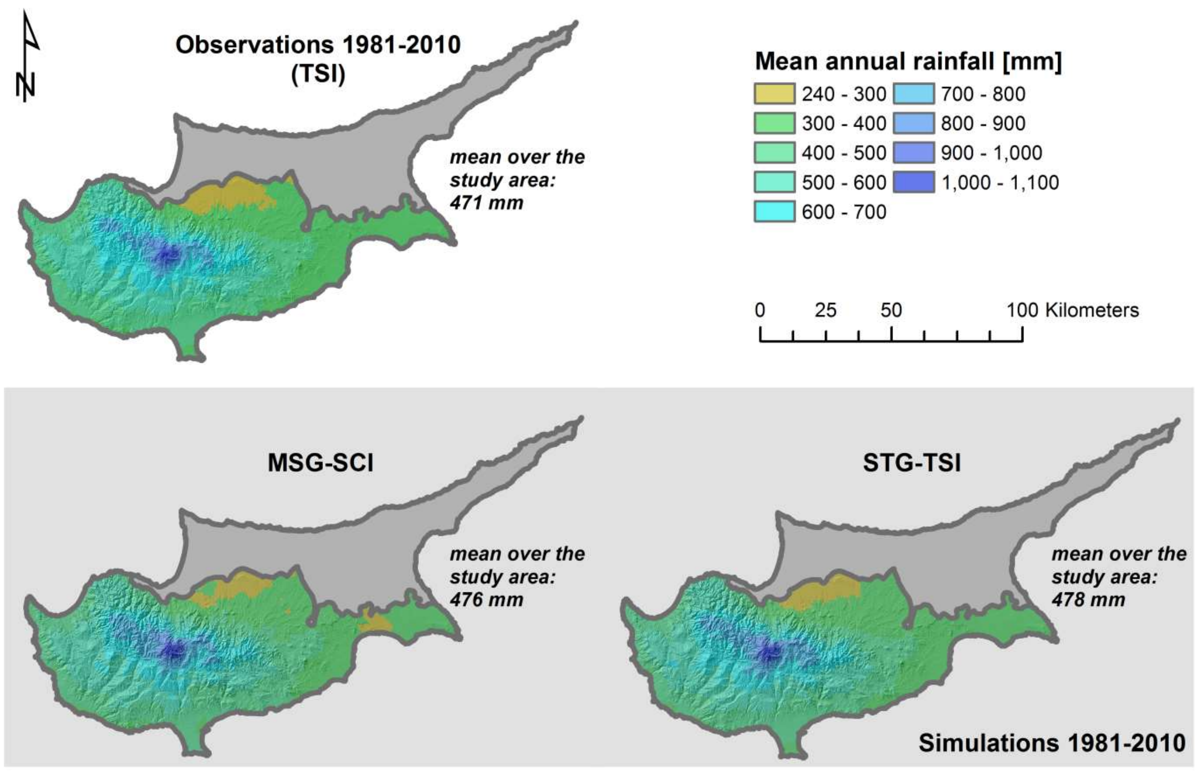

Fig. 9. Mean annual rainfall maps (hydrological years, October-September) calculated for the period 1981-2010 for observations and simulated time series. Observations are interpolated with the two-step method (TSI), as well as the time series simulated with the spatial rainfall generator. Data from the single site generator are interpolated with the scaling coefficient scheme (SCI).

3.3 *Evaluation of future changes*

Because of the failure of the STG method to represent the daily rainfall statistics, future gridded data sets generated with the MSG- TSI method only are presented. The mean annual rainfall values over the country for the reference and future periods are displayed in Fig. 10.

Results obtained with the input data from the three RCMs (CNRM, KNMI, and METO-HC) are shown. For the CNRM model the projected change, for rain gauges, ranges between -189 and +8 mm. The most affected areas, in terms of percentage of rainfall decrease, are the core of the Troodos Mountains and the East coast, while only two stations show a projected increase of mean annual rainfall, in any case lower than 5%. For the KNMI model, the projected changes fall between -101 and +38 mm. In this case, 25 stations project an increase in mean annual rainfall and they are mainly located in the south-eastern foothills of the

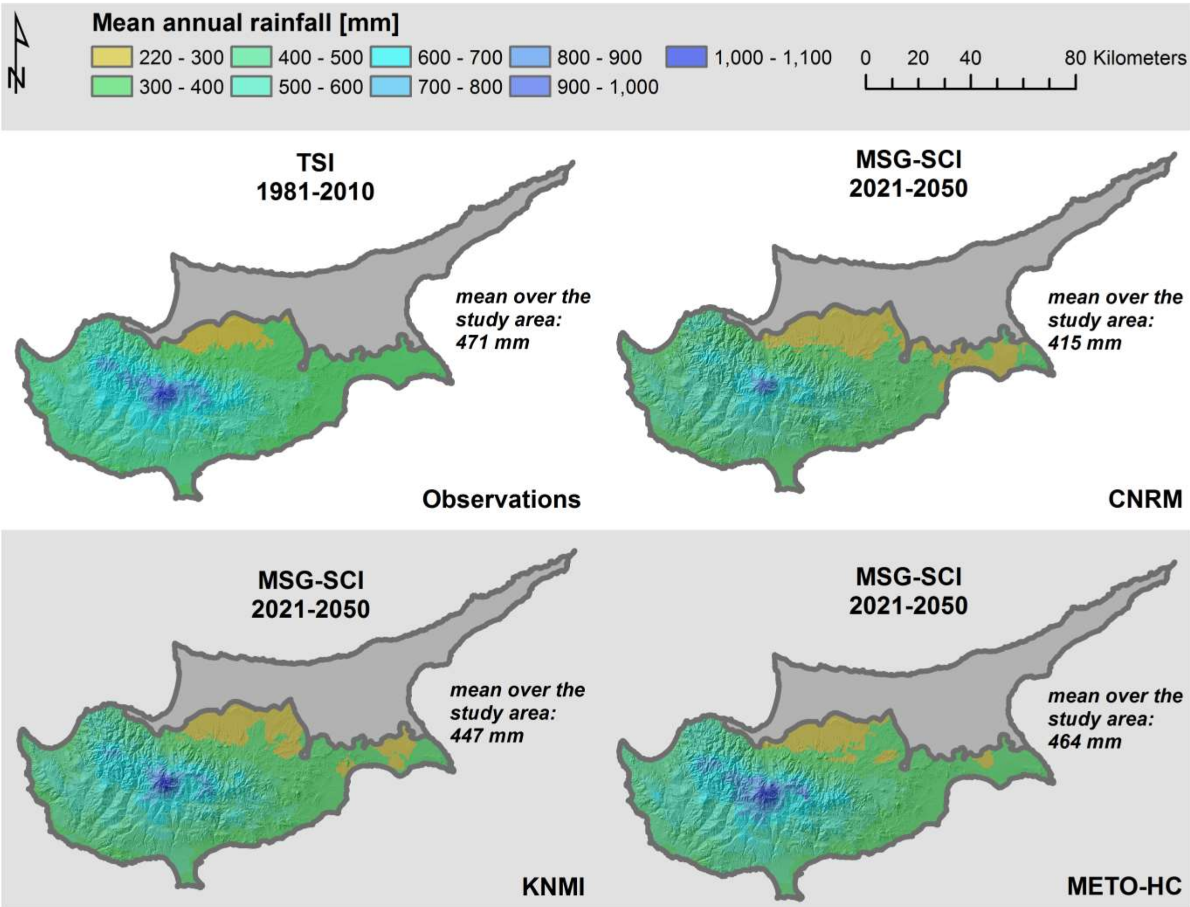

Fig. 10. Mean annual rainfall values for observations (1981-2010) and future projections (2021-2050) calculated from the generated gridded daily data sets (1 x 1 km^2) for hydrological years (October-September). The mean annual precipitation value calculated over the whole country is presented next to each map. TSI refers to the two step interpolation scheme; MSG-SCI indicates the single site rainfall generator and the scaling coefficient interpolation scheme.

Troodos Mountains. The Mesaoria Plain and the East Coast are the areas with the higher projected decreases in mean annual rainfall. Future time series generated with data from the METO-HC model show a very different trend. Indeed, rainfall is projected to increase slightly in the area of the Troodos Mountains and its south-western foothills (maximum increase 77 mm) and to decrease in the Mesaoria Plain (maximum decrease around 68 mm). The projected changes for the five representative stations and the three RCMs are presented in Table 3.

The relative change in the indices R50, RT95, and RA95 for the three future data sets, compared to past observations are presented in Fig. 11. All three downscaled models are generally projecting a decrease in the number of heavy precipitation days (R20) over the country, with an average range between -4% (METO-HC) and -19% (CNRM), therefore beyond the model error, which is (-2%). Projections of two models (CNRM and METO-HC) predict a decreasing R50 as well, while the KNMI model projects a very small increase (2%). It is worth noticing how the IQRs of all future simulations for the R50 index are wider than the IQR for the simulation of the period 1980-2020, indicating different changes in different regions of the country. According to the CNRM model the highest decrease in the number of extremes should occur in the wettest regions, while the other two models project this decrease to be higher in the dry part of the country. Considering that the mean error for this index for the simulation of the control period was around -11%, only the CNRM model projects a change outside the error range of the model (-24%), as well as the KNMI model (+2%)

RT95, RA95, RT99, and RA99 are generally projected to remain fairly constant in comparison with the past. In particular, the METO-HC model projects a future more similar to the past than the other two models. In general, a little higher variability (wider IQRs, longer whiskers and more outliers) can be expected for the RT99 and RA99 indices in comparison to RT95 and RA95. The RA95 and RA99 indices have been derived considering

Table 3 Observed mean annual rainfall (hydrological years, 1981-2010) at 145 rain gauges and projected future (2021-2050) differences (Δ) as for the downscaling of three different RCMs through a multi-single site rainfall generator.

Station ID:	41	225	660	666	731
Location:	Polis	Prodromos	Kornos	Athalassa	Larnaka
Elevation [m a.s.l.]	15	1380	370	162	1
Observed [mm]	415	800	455	319	333
ΔCNRM [mm]	-43	-107	-64	-22	-15
ΔKNMI [mm]	4	-4	-61	-37	-20
ΔMETOHC [mm]	15	-43	-23	6	-2

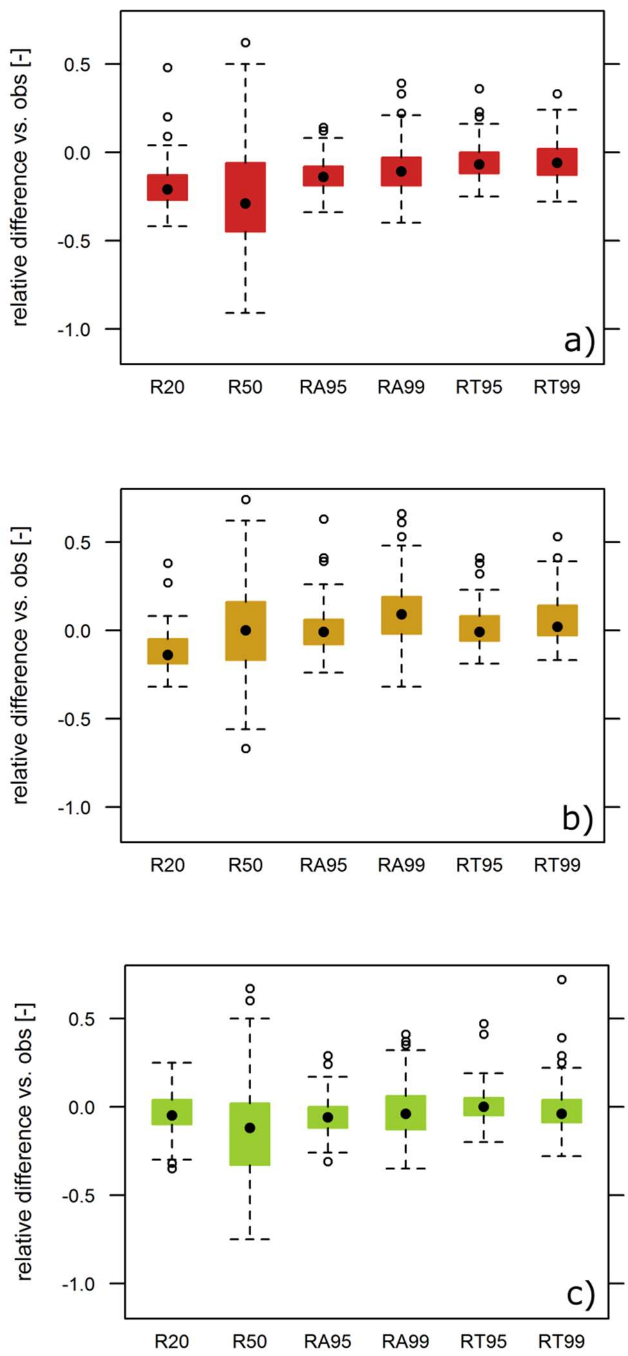

Fig. 11. Relative change in the extremes indices of the observed (1980-2010) and simulated (2020-2050) time series at the 145 rain gauges of a) CNRM, b) KNMI, c) and METO-HC models downscaled with the MSG.

the RT95 and RT99 values calculated for each data set independently. Therefore, a lower RT leads to include, in the calculation of future RA, rainfall events that would not have been considered in the control period. However, the CNRM and METO-HC models project a decrease of these indices: -14% and -9% for CNRM, and -26% and -3% for METO-HC for

RA95 and RA99, respectively. The KNMI model projects no changes in terms of RA95 and a slight increase in RA99 (12%). This last value, together with the CNRM projection for RA95, is the only average over the study area projecting a change beyond the simulation error for the past.

4 Conclusion

Two approaches to generate future time series of daily rainfall based on the statistical downscaling of RCMs outputs were presented. An analysis of projected future climate changes for Cyprus (2020-2050) was carried out as well.

Both a multi-single site and a spatial-temporal rainfall generator (MSG and STG, respectively) were tested. The STG, based on the NSRP model, creates spatially consistent daily maps but is not able to reproduce small scale events (involving less than 10 stations) and underestimates extremes. In particular, the model is completely unable to capture the extreme behaviour of the driest regions of the study area. The problems originate from the orographic complexity of the study area, which leads to very different rainfall regimes over neighbouring regions, and the assumptions and simplifications (rainfall coming as a homogeneous Poisson process) implicit in the model. The NSAR-NSRP model proposed by Burton et al. (2010a), which includes a non-homogeneous spatial activation of rain cells, looks like a promising instrument. On one hand, such a model was proven to be able to well model both non-homogeneous rainfall occurrences, rainfall intermittency, and mean rainfall amounts (Burton et al. 2010a). On the other hand, the modelling of extremes has not yet been thoroughly assessed and further development of the model might be needed. In this sense, alternative approaches like the Bayesian model coupled with an upper-bounded distribution function proposed by Costa et al. (2015), in which the authors simulate extremes separately from the other part of the time series, could be taken into consideration.

In this study, the issue related to the downscaling of precipitation over a complex topographic area has been overcome by the use of a multi-single site generator, which generally models well all the input rainfall statistics and properties, including those related to extremes. However, the main disadvantage of the multi-single site approach is that time series generated at different locations are not correlated to each other. Thus, the downscaled time series are good for the single location but problems arise for the development of spatial data sets. Here, a simplified gridding scheme based on Thiessen polygons and scaling coefficients was presented. The method keeps the water balance over monthly and annual scales for each grid cell and it simulates extremes. The resulting daily maps have no spatial consistency between rainfall amounts falling in different polygons and they cannot be used for applications that need spatial continuity such as distributed hydrological modelling.

Climate change projections were downscaled and gridded with the MSG approach for three different RCMs. In comparison to the control period (1980-2010), mean annual rainfall over the study area is projected to decrease by 1.5% - 12%, according to the three downscaled RCMs. A slight reduction in the number and intensity of extremes is also projected all over the study area. The created data sets are currently being used for climate change impact and adaptation studies for agricultural and environmental applications.

5 Acknowledgments

This study is part of the AGWATER project (ΑΕΙΦΟΡΙΑ/ΓΕΩΡΓΟ/0311(ΒΙΕ)/06), co-financed by the European Regional Development Fund and the Republic of Cyprus through the Research Promotion Foundation.

6 References

Ailliot P, Thomson C, Thomson P (2009) Space-time modelling of precipitation by using a hidden Markov model and censored Gaussian distributions. J R Stat Soc Appl Statist 58:405-426. doi: 10.1111/j.1467-9876.2008.00654.x

Apipattanavis S, Podesta G, Rajagopalan B, Katz RW (2007) A semiparametric multivariate and multisite weather generator. Water Resour Res 43:W11401. doi:10.1029/2006WR005714

Avellan T, Zabel F, Mauser W (2012) The influence of input data quality in determining areas suitable for crop growth at the global scale – a comparative analysis of two soil and climate datasets. Soil Use and Management 28:249–265. doi:10.1111/j.1475-2743.2012.00400.x

Badas MG, Deidda R, Piga E (2006) Modulation of homogeneous space-time rainfall cascades to account for orographic influences. Nat Hazards Earth Syst Sci 6, 427-437. doi:10.5194/nhess-6-427-2006

Baigorria GA, Jones JW (2010) GiST: a stochastic model for generating spatially and temporally correlated daily rainfall data. J Clim 23(22):5990–6008. doi:10.1175/2010JCLI3537.1

Boé J, Terray L, Habets F, Martin E (2007) Statistical and dynamical downscaling of the Seine basin climate for hydro-meteorological studies. Int J Climatol 27:1643–1655. doi:10.1002/joc.1602

Böhm U, Kücken M, Ahrens W, Block A, Hauffe D, Keuler K, Rockel B, Will A (2006) CLM - the climate version of LM: brief description and long-term applications. COSMO Newsletter 6:225–235

Bordoy R, Burlando P (2014) Stochastic downscaling of precipitation to high-resolution scenarios in orographically complex regions: 1. Model evaluation. Water Resour Res 50: 540–561. doi:10.1002/2012WR013289

Borgomeo E, Hall JW, Fung F, Watts G, Colquhoun K, Lambert C (2014) Risk-based water resources planning: Incorporating probabilistic nonstationary climate uncertainties. Water Resour Res 50:6850–6873. doi:10.1002/2014WR015558

Brissette F, Khalili M, Leconte R (2007) Efficient stochastic generation of multisite synthetic precipitation data. J Hydrol 345:121–133. doi:10.1016/j.jhydrol.2007.06.035

Buonomo E, Jones R, Huntingford IC, Hannaford J (2007) On the robustness of changes in extreme precipitation over Europe from two high resolution climate change simulations. Q J Roy Met Soc 133:65–81. doi:10.1002/qj.13

Burton A, Fowler HJ, Blenkinsop S, Kilsby CG (2010b) Downscaling transient climate change using a Neyman-Scott Rectangular Pulses stochastic rainfall model. J Hydrol 381:18–32. doi:10.1016/j.jhydrol.2009.10.031

Burton A, Fowler HJ, Kilsby CG, O'Connell PE (2010a) A stochastic model for the spatial-temporal simulation of non-homogeneous rainfall occurrence and amounts, Water Resour Res 46:W11501. doi:10.1029/2009WR008884

Burton A, Kilsby CG, Fowler HJ, Cowpertwait PSP, O'Connell PE (2008) RainSim: A spatial-temporal stochastic rainfall modelling system. Environmental Modelling & Software 23:1356–1369. doi:10.1016/j.envsoft.2008.04.003

Camera C, Bruggeman A, Hadjinicolaou P, Pashiardis S, Lange MA (2014) Evaluation of interpolation techniques for the creation of gridded daily precipitation (1×1 km^2); Cyprus, 1980–2010. J Geophys Res Atmos, 119:693–712. doi:10.1002/2013JD020611

Caraway NM, McCreight JL, Rajagopalan B (2014) Multisite stochastic weather generation using cluster analysis and k-nearest neighbor time series resampling. J Hydrol 508:197–213. doi:10.1016/j.jhydrol.2013.10.054

Chandler RE, Wheater HS (2002) Analysis of rainfall variability using generalized linear models: a case study from the west of Ireland. Water Resour Res 38:1192. doi:10.1029/2001WR000906

Collins M, Booth BBB, Harris GR, Murphy JM, Sexton DMH, Webb MJ (2005) Towards quantifying uncertainty in transient climate change. Clim Dyn 27:127–147. doi:10.1007/s00382-006-0121-0

Costa V, Fernandes W, Naghettini M 2015. A Bayesian model for stochastic generation of daily precipitation using an upper-bounded distribution function. Stoch Environ Res Risk Assess 29:563–576. doi:10.1007/s00477-014-0880-9

Cowpertwait PSP (1995) A generalized spatial-temporal model of rainfall based on a clustered point process. Proc R Soc London Ser A 450:163–175. doi:10.1098/rspa.1995.0077

Cowpertwait PSP, Kilsby CG, O'Connell PE (2002) A space-time Neyman-Scott model of rainfall: Empirical analysis of extremes. Water Resour Res 38:1131. doi:10.1029/2001WR000709.

Cowpertwait PSP, Ocio D, Collazos G, de Cos O, Stocker C (2013) Regionalised spatiotemporal rainfall and temperature models for flood studies in the Basque Country, Spain. Hydrol Earth Syst Sci 17:479–494. doi:10.5194/hess-17-479-2013

Deidda R, Benzi R, Siccardi F (1999) Multifractal modeling of anomalous scaling laws in rainfall. Water Resour Res 35:1853–1867. doi:10.1029/1999WR900036

Déqué M, Dreveton C, Braun A, Cariolle D (1994) The ARPEGE-IFS atmosphere model: a contribution to the French community climate modelling. Clim Dyn 10: 249–266

Forsythe N, Fowler HJ, Blenkinsop S, Burton A, Kilsby CG, Archer DR, Harpham C, Hashmi M.Z (2014) Application of a stochastic weather generator to assess climate change impacts in a semi-arid climate: The Upper Indus Basin. J Hydrol 517:1019–1034. doi:10.1016/j.jhydrol.2014.06.031

Fowler HJ, Blenkinsop S, Tebaldi C (2007) Linking climate change modelling to impacts studies: recent advances in downscaling techniques for hydrological modelling. Int J Climatol 27:1547–1578. doi:10.1002/joc.1556

Fowler HJ, Kilsby CG, O'Connell PE, Burton A (2005) A weather-type conditioned multi-site stochastic rainfall model for the generation of scenarios of climatic variability and change. J Hydrol 308, 50–66. doi:10.1016/j.jhydrol.2004.10.021

Furevik T, Bentsen M, Drange H, Kindem IKT, Kvamsto NG, Sorteberg A (2003) Description and evaluation of the Bergen climate model: ARPEGE coupled with MICOM. Clim Dyn 21:27–51. doi:10.1007/s00382-003-0317-5

Gires A, Onof C, Maksimovic C, Schertzer D, Tchiguirinskaia I, Simões N (2012) Quantifying the impact of small scale unmeasured rainfall variability on urban runoff through multifractal downscaling: A case study. J Hydrol 442-443:117–128.

Gonçalves M, Barrera-Escoda A, Guerreiro D, Baldasano JM, Cunillera J (2014) Seasonal to yearly assessment of temperatureand precipitation trends in the North WesternMediterranean Basin by dynamical downscaling of climate scenarios at high resolution (1971–2050). Clim Change 122:243–256. doi:10.1007/s10584-013-0994-y

Gosling SN, Lowe·JA, McGregor·GR, Pelling·M, Malamud BD (2009) Associations between elevated atmospheric temperature and human mortality: a critical review of the literature. Clim Change 92:299–341. doi:10.1007/s10584-008-9441-x

Groppelli B, Bocchiola D, Rosso R (2011) Spatial downscaling of precipitation from GCMs for climate change projections using random cascades: A case study in Italy. Water Resour Res 47: W03519. doi:10.1029/2010WR009437

Hadjinicolaou P, Giannakopoulos C, Zerefos C, Lange MA, Pashiardis S, Lelieveld J (2011) Mid-21st century climate and weather extremes in Cyprus as projected by six regional climate models. Reg Environ Change 11:441–457. doi:10.1007/s10113-010-0153-1

Harrold TI, Sharma A, Sheather SJ (2003) A nonparametric model for stochastic generation of daily rainfall amounts. Water Resour Res 39:1–12. doi:10.1029/2003WR002570

Hashmi MZ, Shamseldin AY, Melville BW (2011) Comparison of SDSM and LARS-WG for simulation and downscaling of extreme precipitation events in a watershed. Stoch Environ Res Risk Assess 25:475–484. doi:10.1007/s00477-010-0416-x

Haugen JE, Haakenstad H (2006) Validation of HIRHAM version 2 with 50 km and 25 km resolution. RegClim General Technical Report No 9, pp 159–173

Jacob D (2001) A note on the simulation of the annual and interannual variability of the water budget over the Baltic Sea drainige basin. Meteorol Atmos Phys 77:61–73. doi:10.1007/s007030170017

Khalili M, Brisette F, Leconte R 2009. Stochastic multi-site generation of daily weather data. Stoch Environ Res Risk Assess 23:837–849. doi:10.1007/s00477-008-0275-x

Kilsby CG, Jones PD, Burton A, Ford AC, Fowler HJ, Harpham C, James P, Smith A, Wilby RL (2007) A daily weather generator for use in climate change studies. Environmental Modelling & Software 22:1705–1719. doi:10.1016/j.envsoft.2007.02.005

Kim T, Ahn H, Chung G, Yoo C (2008) Stochastic multi-site generation of daily rainfall occurrence in south Florida. Stoch Environ Res Risk Assess 22:705–717. doi:10.1007/s00477-007-0180-8

Kizza M, Westerberger I, Rodhe A, Ntale HK (2012) Estimating areal rainfall over Lake Victoria and its basin using ground-based and satellite data. J Hydro. 464-465:401–411. doi:10.1016/j.jhydrol.2012.07.024

Kleiber W, Katz RW, Rajagopalan B (2012) Daily spatiotemporal precipitation simulation using latent and transformed Gaussian processes. Water Resour Res 48:1–17. doi:10.1029/2011WR011105

Langousis A, Carsteanu AA, Deidda R (2013) A simple approximation to multifractal rainfall maxima using a generalized extreme value distribution model. Stoch Environ Res Risk Assess 27:1525–1531. doi:10.1007/s00477-013-0687-0

Law AM, Kelton WD (1991). Simulation modelling and analysis. McGraw-Hill, New York, 759 pp.

Lelieveld J, Hadjinicolaou P, Kostopoulou E, Chenoweth J, El Maayar M, Giannakopoulos C, Hannides C, Lange MA, Tanarhte M, Tyrlis E, Xoplaki E (2012) Climate change and impacts in the Eastern Mediterranean and the Middle East. Clim Change 114:667–687. doi:10.1007/s10584-012-0418-4

Lenderink G, van Meijgaard E (2008) Increase in hourly precipitation extremes beyond expectations from temperature changes. Nat Geosci 1:511–514. doi:10.1038/ngeo262.

Marani M (2003) On the correlation structure of continuous and discrete point rainfall. Water Resour Res 39:1128. doi:10.1029/2002WR001456

Maraun D, Wetterhall F, Ireson AM, Chandler RE, Kendon EJ, Widmann M, Brienen S, Rust HW, Sauter T, Themeßl M, Venema VKC, Chun KP, Goodess CM, Jones RG, Onof C, Vrac M, Thiele-Eich I (2010) Precipitation downscaling under climate change: Recent developments to bridge the gap between dynamical models and the end user. Rev Geophys 48:RG3003. doi:10.1029/2009RG000314

Mascaro G, Piras M, Deidda R, Vivoni ER (2013) Distributed hydrologic modeling of a sparsely monitored basin in Sardinia, Italy, through hydrometeorological downscaling. Hydrol Earth Syst Sci 17:4143–4158. doi:10.5194/hess-17-4143-2013

Matlas NC (1967) Mathematical assessment of synthetic hydrology. Water Resour Res 3:937–945. doi:10.1029/WR003i004p00937

McCullagh P, Nelder JA (1989) Generalized linear models. Chapman and Hall, London

McRobie FH, Wang L-P, Onof C, Kenney S (2013) A spatial-temporal rainfall generator for urban drainage design. Water Sci Technol 68:240–249. doi: 10.2166/wst.2013.241

Mehrotra R, Li J, Westra S, Sharma A (2015) A programming tool to generate multi-site daily rainfall using a two-stage semi parametric model. Environmental Modelling & Software 63:230–239. doi:10.1016/j.envsoft.2014.10.016

Mehrotra R, Sharma A, Cordery I (2004) Comparison of two approaches for downscaling synoptic atmospheric patterns to multi-site precipitation occurrence. J Geophys Res Atmos 109:D14107. Doi:10.1029/2004JD004823

Mehrotra R, Srikanthan R, Sharma A (2006) A comparison of three stochastic multi-site precipitation occurrence generators. J Hydrol 331:280–292. doi:10.1016/j.jhydrol.2006.05.016

Michaelides SC, Tymvios FS, Michaelidou T (2009) Spatial and temporal characteristics of the annual rainfall frequency distribution in Cyprus. Atmos Res 94:606–615. doi:10.1016/j.atmosres.2009.04.008

Molnar P, Burlando P (2008) Variability in the scale properties of high-resolution precipitation data in the Alpine climate of Switzerland. Water Resour Res 44:W10404. doi:10.1029/2007WR006142

Moron V, Robertson AW, Ward MN, and Ndiaye O (2008) Weather types and rainfall over Senegal. Part II: Downscaling GCM simulations. J Clim 21:288–307. doi:10.1175/2007JCLI1624.1

Olsson J, Burlando P (2002) Reproduction of temporal scaling by a rectangular pulses rainfall model. Hydrol Process 16: 611–630. doi:10.1002/hyp.307

Parkes BL, Wetterhall F, Pappenberger F, He Y, Malamud BD, Cloke HL (2013) Assessment of a 1-hour gridded precipitation dataset to drive a hydrological model: a case study of the summer 2007 floods in the Upper Severn, UK. Hydrol Res 44:89–105. doi:10.2166/nh.2011.025

Perica S, Foufoula-Georgiou E (1996) Model for multiscale disaggregation of spatial rainfall based on coupling meteorological and scaling descriptions. J Geophys Res Atmos 101:26347–26361. doi:10.1029/96JD01870

Prudhomme C, Reynard N, Crooks S (2002) Downscaling of global climate models for flood frequency analysis: Where are we now? Hydrol Process 16:1137–1150. doi:10.1002/hyp.1054

Radu R, Déqué M, Somot S (2008) Spectral nudging in a spectral regional climate model. Tellus Ser A 60:898–910. doi:10.1111/j.1600-0870.2008.00341.x

Rodrigues-Iturbe I, Cox DR, Isham V (1987) Some models for rainfall based on stochastic point processes. Proc R Soc Lond Ser A 410:269–288. doi:10.1098/rspa.1987.0039

Roeckner E, Bauml G, Bonaventura L, Brokopf R, Esch M, Giorgetta M, Hagemann S, Kirchner I, Kornblueh L, Manzini E, Rhodin A, Schlese U, Schulzweida U, Tompkins A (2003) The atmospheric general circulation modell ECHAM5, part I: model description. Tech Rep 349, Max-Planck-Institute for Meteorology, Hamburg, Germany

Rummukainen M (2010) State-of-the-art with regional climate models. WIREs Clim Change 1:82–96. doi:10.1002/wcc.8

Simões N, Ochoa-Rodríguez S, Wang LP, Pina R, Sa Marques A, Onof C, Leitão J (2015) Stochastic Urban Pluvial Flood Hazard Maps Based upon a Spatial-Temporal Rainfall Generator. Water 7:3396–3406. doi:10.3390/w7073396

Supit I, van Diepen CA, de Wit AJW, Wolf J, Kabat P, Baruth B, Ludwig F (2012) Assessing climate change effects on European crop yields using the Crop Growth Monitoring System and a weather generator. Agricult Forest Meteorol 164:96–111. doi:10.1016/j.agrformet.2012.05.005

van der Linden P, Mitchell JFB (2009) ENSEMBLES: climate change and its impacts. Summary of research and results from the ENSEMBLES project. Met Office Hadley Centre, Exeter. Available at: http://ensembles-eu.metoffice.com/docs/Ensembles_final_report_Nov09.pdf (2009). Accessed 22 September 2014

Van Vilet MTH, Blenkinsop S, Burton A, Harpham C, Broers HP, Fowler HJ (2012) A multi-model ensemble of downscaled spatial climate change scenarios for the Dommel catchment, Western Europe. Clim Change 111:249–277. doi:10.1007/s10584-011-0131-8

Veneziano D, Furcolo P, Iacobellis V (2006) Imperfect scaling of time and space-time rainfall. J Hydrol 322:105–119. doi:10.1016/j.jhydrol.2005.02.044

Venugopal V, Roux SG, Foufoula-Georgiou E, Arneodo A. (2006) Revisiting multifractality of high-resolution temporal rainfall using a wavelet-based formalism. Water Resour Res 42:W06D14. doi:10.1029/2005WR004489

Verdin A, Rajagopalan B, Kleiber W, Katz RW (2015) Coupled stochastic weather generation using spatial and generalized linear models. Stoch Environ Res Risk Assess 29:347–356. doi:10.1007/s00477-014-0911-6

Wilks DS (1998) Multisite generalization of a daily stochastic precipitation generation model. J Hydrol 210:178–191. doi:10.1016/S0022–1694(98)00186-3

Wilks DS (2009). A gridded multisite weather generator and synchronization to observed weather data. Water Resour Res 45:W10419. doi:10.1029/2009WR007902

Willems P (2001) A spatial rainfall generator for small spatial scales. J Hydrol 252:126–144. doi:10.1016/S0022-1694(01)00446-2

Yang C, Chandler RE, Isham VS, Wheater HS (2005) Spatial-temporal rainfall simulation using generalized linear models. Water Resour Res 41:W11415. doi:10.1029/2004WR003739

Yates D, Gangopadhyay S, Rajagopalan B, Strzepek K (2003) A technique for generating regional climate scenarios using a nearest-neighbor algorithm. Water Resour Res 39:1199. doi:10.1029/2002WR001769,

Zhang X, Aguilar E, Sensoy S et al (2005) Trends in Middle East climate extreme indices from 1950 to 2003. J Geophys Res Atmos 110:D22104. doi:10.1029/2005JD006181